Supporting Information

Acid deprotonation driven by cation migration at biased graphene nanoflake electrodes

Mailis M. Lounasvuori and Katherine B. Holt*

Department of Chemistry, University College London, 20 Gordon St, London WC1H 0AJ

Contents:

S1. Derivation of Equation 1

For an acid *HA*:

$$HA = H^+ + A^- \qquad\qquad K_a = \frac{a_{H^+}\, a_{A^-}}{a_{HA}} \qquad\qquad \text{(Eq. S1)}$$

However, if excess cation M^+ is present, this can associate with A^- and change its activity:

$$M^+ + A^- = A^-(M^+) \qquad K_{as} = \frac{a_{A^-(M^+)}}{a_{M^+}\, a_{A^-}} \text{ and therefore: } a_{A^-} = \frac{a_{A^-(M^+)}}{K_{as}\, a_{M^+}} \qquad \text{(Eq. S2)}$$
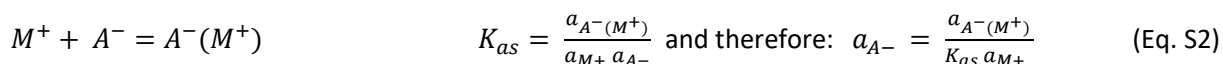
Substituting Eq. S2 into Eq. S1:

$$K_a = \frac{a_{H^+} a_{A^-(M^+)}}{a_{HA} K_{as} a_{M^+}}$$

Taking logs:

$$\log K_a = \log \frac{a_{H^+} a_{A^-(M^+)}}{a_{HA}} - \log K_{as} - \log a_{M^+} \qquad \text{(Eq. S3)}$$

By definition, the first term in Eq. S3 is *–pK$_a$(app)* – the measured pK$_a$ when the activity of A^- differs from that of 'free' A^- due to the presence of M^+.

Therefore:

$$-pK_a = -pK_a(app) + pK_{as} - \log a_{M^+} \qquad \text{which rearranges to Eq. 1.}$$

S2. Experimental methods

S2.1 Preparation of complexed GNF

For preparation of GNF complexed with divalent cations 3.3 mg of GNF dissolved in deionized water was neutralized with dilute KOH to deprotonate all acidic groups. An aqueous solution of $CaCl_2$ was added dropwise and the mixture was agitated between additions. The resulting precipitate suspension was centrifuged and washed four times. The precipitate was then resuspended in water and sonicated briefly before each use. The concentration of the suspension, assuming full conversion of GNF and one Ca^{2+} per two carboxylate groups, is estimated to be (5 ± 1) mg/ml.

S2.2 Electrode preparation

A 3 mm diameter boron-doped diamond (BDD) disk sealed in PEEK (Windsor Scientific) was used as the working electrode, either unmodified or modified with a layer of adsorbed GNF. A platinum wire served as a counter electrode. The reference electrode was Ag/AgCl in saturated KCl and all potentials are reported relative to it. The GNF samples were drop-cast from aqueous suspensions of known concentration onto the freshly polished BDD electrode using a micropipette and allowed to dry under ambient conditions. After drying, the electrode was rinsed thoroughly with ultrapure water to remove any poorly adhered material from the surface and dried using an ambient air flow. The amount of GNF-Ca deposited on the electrode is estimated to be (18 ± 4) × 10^{-6} g.

S2.3 Spectroelectrochemical experiments

In-situ spectroelectrochemical experiments were performed using a Bruker Tensor 27 spectrometer (Bruker, United Kingdom) fitted with a room temperature DLaTGS detector at 4 cm^{-1} resolution and a diamond crystal as the internal reflection element. The potential was controlled with a Palmsens Emstat2 potentiostat (Palmsens, NL) running PSTrace (v3.0) software. An electrochemical cell with a volume of 2 ml was positioned over the ATR element. The electrodes used are as detailed above. Experiments were carried out in background electrolyte solutions of different pH in the range 3.0 to 9.2, which were prepared by mixing different

proportions of 0.1 M solutions of KH_2PO_4, K_2HPO_4, H_3PO_4, Na_2SO_4, H_2SO_4, HCl, KCl, KOH and NaOH. The pH of the electrolyte was checked with a pH meter.

The GNF-Ca electrode was equilibrated in the electrolyte for *ca*. 30 min then an IR background spectrum obtained. A potential of +1.0 V was applied and spectra recorded relative to spectrum of the equilibrated sample. A background spectrum of the electrode at +1.0 V was then obtained and the potential switched to −0.5 V and spectra measured relative to that at +1.0 V. Three full potential cycles (+1 V followed by −0.5 V) were recorded to assess the reproducibility of the response. A single spectrum was computed by Fourier transformation of 100 averaged interferograms for background and sample and the software was programmed to record a spectrum every 170 seconds. One potential step was 720 seconds in duration, during which time four sample spectra and one background spectrum were recorded. After the initial sample spectrum, the subsequent three spectra were consistently of similar intensity, indicating that the changes upon polarization stabilized after about three minutes and remained stable for at least another 10 minutes. The three spectra from each potential step were processed using the atmospheric compensation function of OPUS software and averaged; the averaged spectra are those presented throughout this work.

S3. Characterization of Graphene Nanoflakes (GNF) and GNF-Ca

The work presented here was conducted using graphene nanoflakes (GNF) provided by Dr Christoph Salzmann (UCL Chemistry) who has previously reported the synthesis and characterization of this novel graphene-related nanomaterial (Rosillo-Lopez, M., Lee, T. J.; Bella, M.; Hart, M.; Salzmann, C. G. *RSC Adv.* **2005**, 5, 104198). ^{13}C solid state NMR studies show that only COOH and sp^2-hybridized carbon are present, indicating that the GNF contain few oxygenated defects on the basal plane and that the oxygen content is concentrated around the edges. High-resolution XPS spectra of the C1s region showed the presence of COOH groups but a complete lack of any alcohol or epoxide groups in GNF, providing further evidence that the GNF consist of a pristine basal plane with carboxylic acid groups decorating the edges.
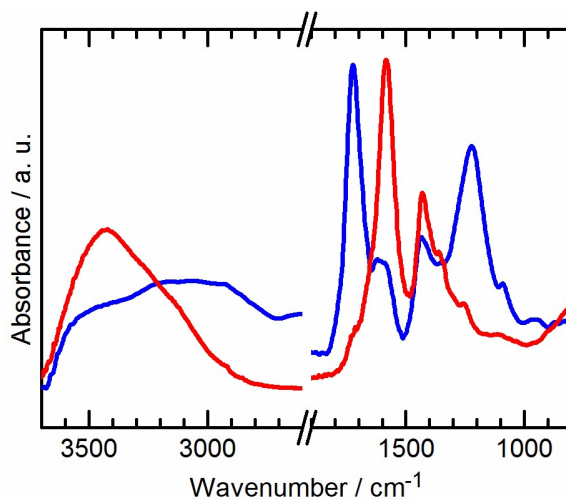
Figure S3.1:   ATR-FTIR spectra of dry GNF-COOH (blue) and dry GNF-Ca (red).

The IR spectrum of dry GNF (Figure S, blue) shows a strong band at 1720 cm^{-1} assigned to the C=O stretching mode of carboxylic acid. Also present are the carboxylate asymmetric stretch at 1580 cm^{-1} and overlapping bands at 1435 and 1350 cm^{-1} assigned to the symmetric carboxylate stretch. The feature at around 1220 cm^{-1} is a convolution of vibrational modes, but can be assigned partly to the C-O stretch in protonated COOH. The broad absorption features at 3700 – 2700 cm^{-1} are attributed to -OH stretches of adsorbed water (> 3000 cm^{-1}) and -OH stretches of the carboxylic acid edge groups (< 3000 cm^{-1}). The persistence of the water band even after

lengthy drying suggests water is strongly associated with the GNF, most likely due to hydrogen bonding to the oxygenated edge groups.

The IR spectrum of the dried GNF-Ca precipitate is also presented in Figure S (red). The most intense peak at 1585 cm^{-1} is assigned to the asymmetric stretch in carboxylate and also contains a contribution from the bending mode of water at 1635 cm^{-1}; this peak is accompanied by the slightly weaker carboxylate symmetric stretch modes at 1430 and 1350 cm^{-1}. The prominence of the carboxylate bands is consistent with carboxylate groups being mostly deprotonated and partially complexed with Ca^{2+}. In order to form a complex with the cation, the carboxylate groups need to exist in a favorable orientation and therefore it is expected that a number of acid groups will remain non-complexed. The C=O stretching band at 1720 cm^{-1} and the C-O stretch at 1220 cm^{-1} are weaker in GNF-Ca than GNF-COOH but clearly visible, confirming that a considerable number of COOH groups are still present in GNF-Ca. The broad absorption band for acid -OH groups at 3000 – 2700 cm^{-1} is reduced compared to the non-complexed GNF, which is consistent with the majority of acid groups being found as carboxylate and/or bound to Ca^{2+}. The presence of a strong stretching band for water at 3700 – 3000 cm^{-1} suggests that, like in GNF-COOH, a significant number of water molecules remain in the sample.

S4. Estimating the distance between the electrode surface and the ATR prism

In the experimental setup, the working electrode surface is located close above the ATR prism, trapping a small amount of solution. The setup can therefore be considered as a thin-layer cell and the special conditions of diffusion can be exploited in estimating the distance between the electrode surface and the ATR element (Faulkner, L. R., Electrochemical characterization of chemical systems. In *Physical methods in modern chemical analysis*, Kuwana, T., Ed. Academic Press: New York, 1983; Vol. 3, pp 137-248). When the thickness of solution is less than about 50 μm, diffusion can homogenize the solution continuously so that concentration gradients do not exist. Provided that the potential scan rates are slow enough to maintain a homogeneous solution, mass transfer effects can be ignored. Theoretical cyclic voltammetric responses in a thin-layer cell will therefore show identical peak potentials for the forward and reverse scans, and peak currents that depend linearly on the scan rate. The peak current is

$$i_p = n^2 F^2 v V C_O^* / 4RT \qquad \text{(Eq. S4)}$$

where n is the number of electrons transferred, F the Faraday constant, v the scan rate, V the volume of the thin layer, C_O^* the initial concentration of species O, R the gas constant and T the temperature. Ferrocenemethanol (FcMeOH) was chosen as the redox probe as it is well known to undergo a reversible, one-electron, outer-sphere redox reaction. The volume of the thin-layer cell is modelled as a cylinder with dimensions A × h, where A is the area of the BDD with radius 1.5 mm and h is the distance to be determined. To eliminate height differences resulting from the ATR prism not being exactly flush with the base plate, a glass cover slip (diameter 15 mm) was placed at the bottom of the cell. From 6 CVs, with scan rates between 5 and 17 mV s^{-1}, the volume was calculated to be 122 ± 4 nl, giving h *ca.* 17 μm.
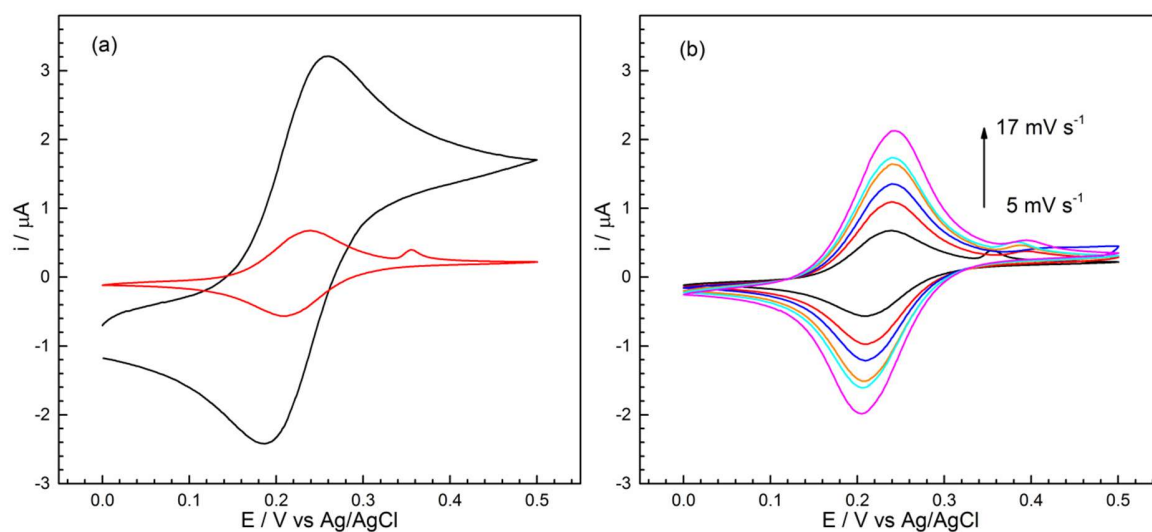
Figure S4.1: Cyclic voltammograms of 1.13 mM FcMeOH in O.1 M NaCl in IR setup. (a) Black line: BDD positioned 5 mm above ATR prism. Red line: BDD positioned against ATR prism, creating thin-layer conditions. Scan rate 5 mV s⁻¹. (b) CVs recorded in the thin-layer geometry with scan rates 5, 8 10, 12, 14 and 17 mV s⁻¹.

Table S4.1. Scan rates, peak currents for forward and backward scans and calculated volumes for thin-layer cell.

v / mV s^{-1}	ip / μA	V / 10^{-9} l
5	0.65	120
5	−0.67	123
8	1.06	123
8	−1.08	125
10	1.33	123
10	−1.37	127
12	1.58	122
12	−1.64	126
14	1.73	114
14	−1.77	117
17	2.15	117
17	−2.18	119

Supporting Information

S5. Penetration depth of IR evanescent wave

In the attenuated total reflection mode, the infrared beam is incident at a crystal made of a material with a high refractive index such as diamond. The sample is placed in contact with the crystal on the other side of the infrared beam. At angles above the so-called critical angle, total reflection of the light occurs, and an evanescent wave forms that extends into the sample. The penetration depth is the distance where the amplitude of the electric field is 1/e of its value at the surface and is given by

$$d_p = \frac{\lambda}{2\pi(n_1^2 \sin^2\theta - n_2^2)^{1/2}}$$

(Eq. S5)

where λ is wavelength, θ is the angle of incidence of the IR beam and n_1 and n_2 are the refractive indices of the crystal and the sample, respectively. The volume of the evanescent wave can be used to compare sample absorbance in ATR mode to that in transmission mode and hence gain quantitative information about the sample. This volume, known as the effective penetration, d_e, is unique for parallel and perpendicular polarization and they are given by:

$$d_{e\perp} = \frac{n_1^2 n_2 \cos\theta}{(n_1^2 - n_2^2)} \cdot \frac{\lambda}{\pi\sqrt{n_1^2 \sin^2\theta - n_2^2}}$$

(Eq. S6)

$$d_{e\parallel} = \frac{n_1^2 n_2 \cos\theta}{(n_1^2 - n_2^2)} \cdot \frac{2n_1^2 \sin^2\theta - n_2^2}{(n_1^2 - n_2^2)\sin^2\theta - n_2^2} \cdot \frac{\lambda}{\pi\sqrt{n_1^2 \sin^2\theta - n_2^2}}$$

(Eq. S7)

d_e for an unpolarized beam is given by

$$d_e = \frac{d_{e\perp} + d_{e\parallel}}{2}$$

(Eq. S8)

Taking diamond as the crystal, pure water as the sample and $\theta = 45°$, values of d_p and d_e were calculated at different wavenumbers and listed in Table S5.1.

Table S5.1. Penetration depth d_p and the effective penetration d_e calculated at different wavenumbers. Values of n_1 were found in (Phillip, H. R.; Taft, E. A., *Physical Review* 1964, *136* (5A), A1445-A1448) and n_2 in (Hale, G. M.; Querry, M. R., *Appl. Opt.* 1973, *12* (3), 555-563).

n_1	n_2	$\tilde{\nu}$ / cm^{-1}	d_p / μm	d_e / μm
2.38	1.22	1000	1.37	2.03
2.38	1.33	1400	1.10	1.91
2.38	1.33	1670	0.92	1.59
2.38	1.33	2000	0.77	1.34
2.38	1.35	2500	0.63	1.13
2.38	1.43	3000	0.60	1.20

The penetration depths were calculated above using pure water as the sample. The refractive index of water will depend on the amount of dissolved ions and n_2 will therefore be slightly different for an electrolyte solution. Berlind's group have measured the effect of ion concentration on refractive indices of fluids (Berlind, T.; Pribil, G. K.; Thompson, D., et al., P*hysica Status Solidi (c)* **2008,** *5* (5), 1249-1252) at wavelengths in the range 0.93 – 5.93 eV, and their results can be used to estimate the change in d_p at wavelengths relevant to this study. They found that at 0.93 eV (7500 cm^{-1}) n changed by 0.01 units for every 1 M change in ion concentration, which translates to a maximum increase in d_p of 2% when the ionic strength changes from 0 to 1 M. Similar estimates can be made based on data reported in (Shippy, B. A.; Burrows, G. H., *J. Am. Chem. Soc.* **1918,** *40* (1), 185-187) and (West, C. J.; Hull, C., *International critical tables of numerical data, physics, chemistry and technology, 1933*. 1st electronic ed.; Knovel: Norwich, NY, 2003).

S6. Comparison of spectral response in oxygenated and deoxygenated electrolyte
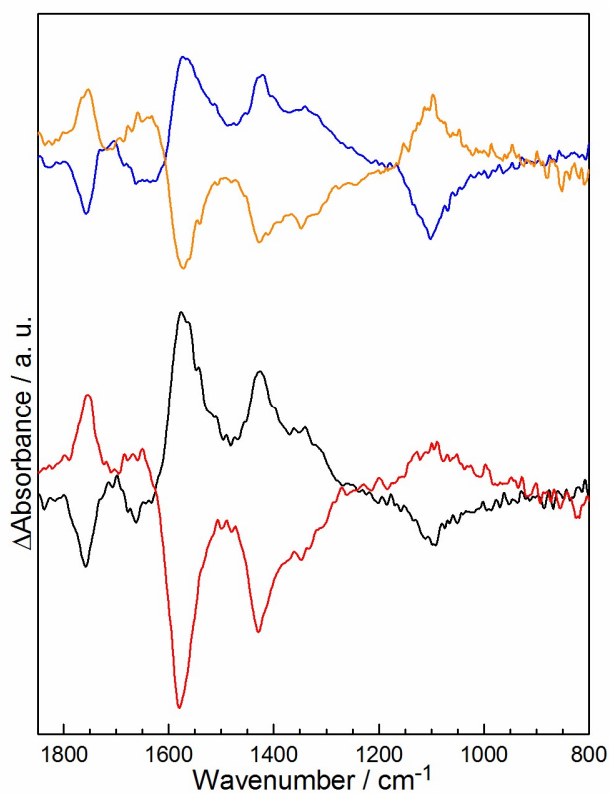
Figure S6. 1 Difference spectra of BDD modified with GNF-Ca in 0.1 M K₂SO₄ pH 3.5. Application of −0.5 V (black); application of +1 V (red). Difference spectra under same conditions but electrolyte deoxygenated with argon for 20 minutes. Application of −0.5 V (blue); application of +1 V (orange).

S7. Spectral response on initial application of +1.0 V
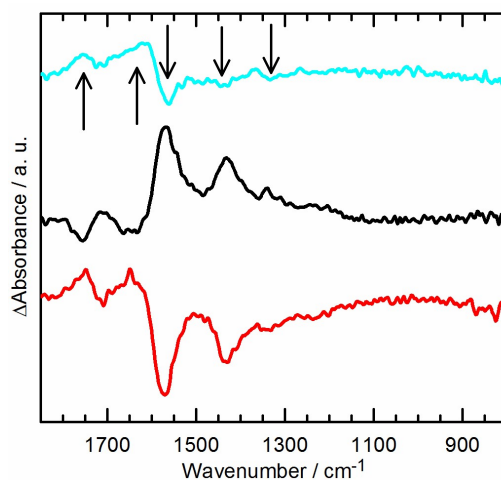
Figure S7.1 Difference spectra of BDD modified with GNF-Ca in 0.1 M NaCl electrolyte at pH 3.5. Initial application of +1 V, background spectrum recorded without applied potential (light blue); spectrum after subsequent application of −0.5 V (black); spectrum after subsequent application of +1 V (red). Arrows on top spectrum indicate direction of spectral features relative to baseline as a guide to the eye.

Figure S7.1 shows the response when the first potential of +1 V is applied to the GNF-Ca modified electrode (light blue) after the background is collected at after 30 min at equilibrated state without applied potential. There are weak losses at 1570 cm^{-1}, 1430 cm^{-1} and 1340 cm^{-1} assigned to carboxylate stretches and gains at 1755 cm^{-1} and 1635 cm^{-1} assigned to the C=O band and water bending mode, respectively. When −0.5 V is applied, a large increase in the intensity of observed features occurs (Fig S7. 1, black). Subsequent application of +1 V (Fig S7.1, red) leads to features that are a mirror image both in intensity and in frequency to those observed at −0.5 V. This set of spectra show that initial application does not result in much change in the protonation state of the GNF-Ca edge groups and that application of −0.5 V is required to induce the first deprotonation step.

S8. Electric field induced deprotonation of electrode-bound acids

Previous studies (refs 1,2 in main manuscript) have found that protonation of electrode-immobilized acids takes place on application of negative electrode potential. This was explained by the relationship between $pK_a(app)$ and surface potential φ given in Eq. S9:

$$pK_a(app) = pK_a - \frac{F\,\varphi}{2.3\,R\,T} \qquad \text{Eq. S9}$$

Eq. S9 therefore predicts that when a negative electrode potential is applied (φ is negative), a positive shift in $pK_a(app)$ will take place. This will result in protonation of any deprotonated acids.

We observe the opposite trend: deprotonation on application of negative potential. The reason for different reported behavior of electrode-immobilized acids seems to be related to the distance between the acid groups and the underlying electrode. Acids located closer to the electrode (e.g. on short chain SAMs) are under a greater influence of the electric field and therefore respond as predicted by equation S9. A mixture of behaviors is reported for longer chain SAMs and more disordered systems. The acids respond either to the change in surface potential of the electrode, or to the change in cation activity (as we describe) depending on how closely they are bound to the electrode and on the local environment. For example, acid groups buried within hydrophobic alkyl chains of SAMs respond to the electrode field, while acids further from the electrode and in contact with solution are more likely to respond to changes in solution conditions than changes to surface potential.

S9. Effect of solution ionic strength on spectral response
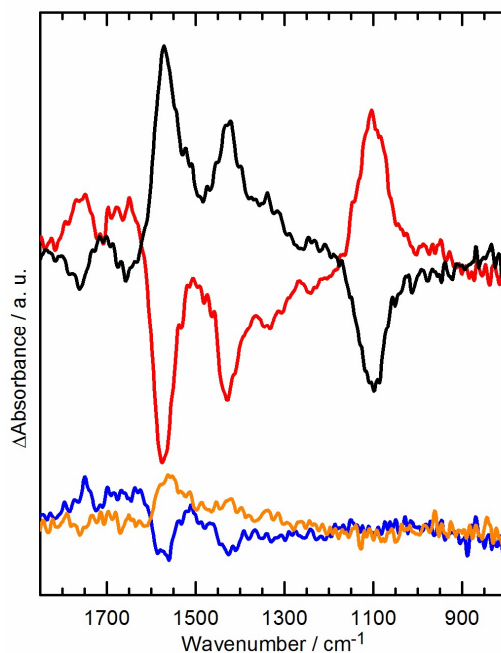
Figure S9.1 Difference spectra in different concentrations of background electrolyte. BDD modified with GNF-Ca in 0.1 M Na$_2$SO$_4$: application of −0.5 V (black); application of +1 V (red). BDD modified with GNF-Ca in 1×10^{-3} M Na$_2$SO$_4$: application of −0.5 V (orange); application of +1 V (blue). Solution pH was 6.8.
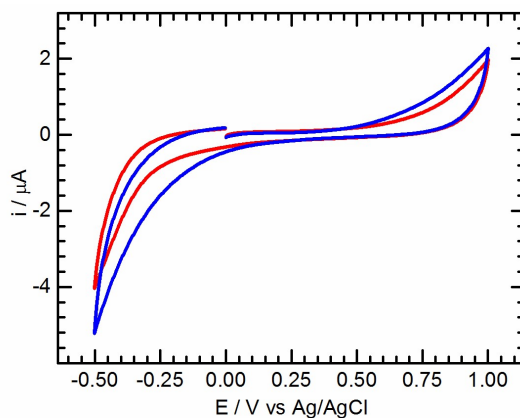
Figure S9.2 Cyclic voltammograms in different ionic strength solutions. BDD modified with GNF-Ca in 1 × 10^{-3} M (red); in 0.1 M PBS at pH 7 (blue).

CV response in different ionic strength solutions is very similar (within variation of repeated experiments under the same conditions), indicating that additional redox chemistry that could result in pH change (O_2, H^+ or water reduction) does not proceed at a significantly different rate at lower ionic strength. In contrast, spectral response (Fig S9 1) is very different in lower ionic strength solution, indicating that ion activity rather than pH change or redox chemistry must be responsible for the observed changes.

S10. Ionic strength of the different solutions used in study

The molar ionic strength I_c of a solution with dissolved ions is given by Equation S10:

$$I_c = \frac{1}{2} \sum_{i=1}^{n} c_i z_i^2$$

Eq. S10

where c_i and z_i are the concentration and charge, respectively, of species i.

Table S10.1. Ionic strengths of sulfate electrolytes used in this study.

	$[K^+]$	$[H^+]$	$[SO_4^{2-}]$	$[HSO_4^-]$	I_c / M
0.1 M pH 3 K_2SO_4	0.192	0.001	0.092	0.008	0.285
0.1 M pH 3.5 K_2SO_4	0.196	3.16×10^{-4}	0.097	0.0026	0.295
0.1 M pH 7 K_2SO_4	0.2		0.1		0.3
1×10^{-3} M pH 7 K_2SO_4	2×10^{-3}		1×10^{-3}		3×10^{-3}

Table S10.2. Ionic strengths of phosphate electrolytes used in this study.

	$[K^+]$	$[H^+]$	$[OH^-]$	$[HPO_4^{2-}]$	$[H_2PO_4^-]$	$[H_3PO_4]$	I_c / M
0.1 M pH 3 phosphate	0.080	1×10^{-3}			0.088	0.012	0.084
0.1 M pH 7 phosphate	0.15			0.039	0.061		0.125
0.1 M pH 9 phosphate	0.2		1×10^{-5}	0.099	0.001		0.15

Thus it can been seen that all solutions used for the results reported in the main manuscript have an ionic strength of the same order of magnitude ca. 0.1 - 0.3 M.

S11. Effect of electrolyte cation on spectral response

The effect of electrolyte cation in potential-dependent acid ionization was investigated. Difference spectra recorded in both 0.1 M Na_2SO_4 and 0.1 M K_2SO_4 at pH 6.8 (Fig S10.1) show that both K^+ and Na^+ cause nearly identical changes to the protonation state of the electrode-immobilized acid groups. The sulfate bands are of equal size, suggesting that the local increase in cation activity is very similar for both K^+ and Na^+.
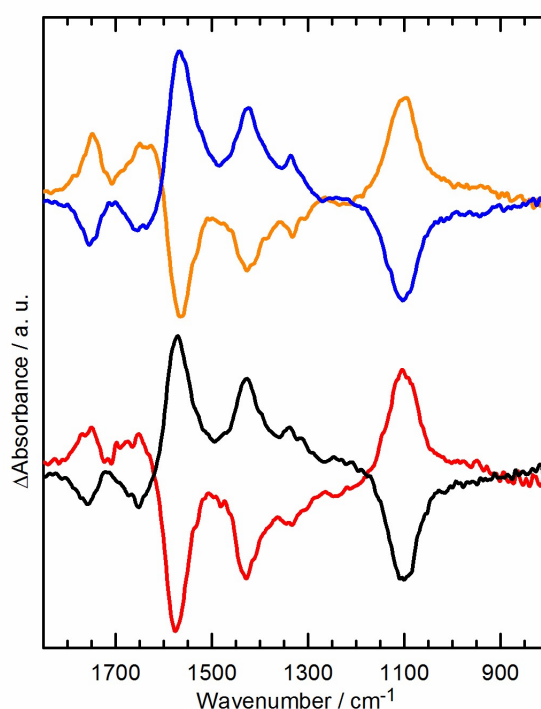
Figure S11.1 Difference spectra of BDD modified with GNF-Ca in 0.1 M K_2SO_4 pH 6.8; application of −0.5 V (black); subsequent application of +1 V (red). Difference spectra of BDD modified with GNF-Ca in 0.1 M Na_2SO_4 pH 6.8; application of −0.5 V (blue); subsequent application of +1 V (orange).

S12. Quantifying changes in sulfate ion concentration on application of −0.5 V

IR spectra of different concentrations of aqueous K_2SO_4 were recorded with the clean ATR element as background and the sulfate absorption peaks were fitted using a Gaussian peak shape. The peak areas were plotted against sulfate concentration and the data points were fitted

with a linear equation to obtain a calibration curve. The intercept was fixed to zero to ensure physically meaningful estimations of small numbers of moles from the calibration curve.

Fig S12.1 a shows IR spectra of different concentrations of aqueous K_2SO_4 and the inset shows the sulfate absorption band at 1100 cm^{-1}. In Fig S12.1 b the peak fitting is illustrated for 0.075 M solution. The peak areas were then plotted against concentration and the data points were fitted with a linear regression line (Fig S12.1 c).

Difference spectra recorded under potential control in 0.1 M K_2SO_4 electrolyte pH 6.8 were fitted with Gaussian peaks as shown in Fig S12.2 and the linear fit equation was used to calculate the change in sulfate ion concentration at the electrode from the sulfate peak area. It was found that the sulfate ion concentration changes by $(-3.5 \pm 0.4) \times 10^{-3}$ M when the potential is changed from +1 V to −0.5 V.
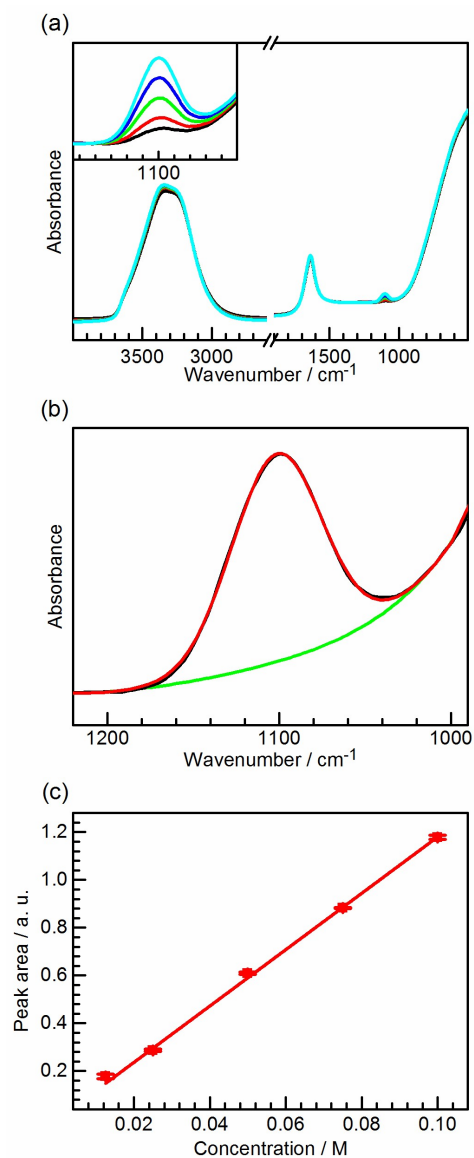
Figure S12.1 (a) Infrared spectra of aqueous solutions of K$_2$SO$_4$ at different concentrations. Inset: Magnification of the SO$_4^{2-}$ absorption bands. (b) Peak fit of the sulfate absorption band from 0.075 M K$_2$SO$_4$ spectrum. Experimental data (black), background curve (green), peak fit (red). (c) Peak areas from (a) plotted against concentration of K$_2$SO$_4$ and a linear fit of data points.
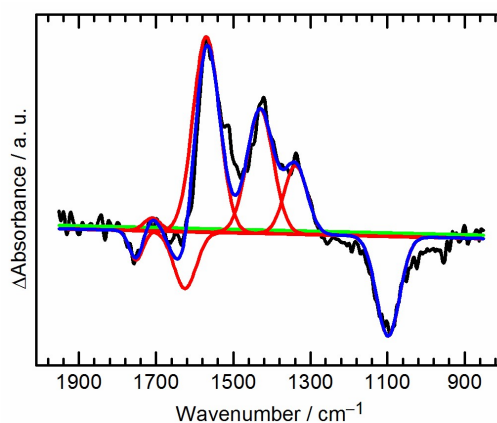
Figure S12.2 Peak fitted difference spectrum in 0.1 M K$_2$SO$_4$ pH 6.8 when applying −0.5 V to GNF-Ca modified BDD. Experimental data (black), background curve (green), peak fits (red), cumulative peak fit (blue).

Table S12.1 Peak areas from difference spectra obtained at different potentials and the calculated concentration change in sulfate ion at the electrode surface.

Potential / V	Conditions	Peak area	Concentration / M
1	0.1 M K$_2$SO$_4$ with O$_2$	0.04089	0.0035
−0.5	0.1 M K$_2$SO$_4$ with O$_2$	−0.04092	−0.0035
1	0.1 M K$_2$SO$_4$ with O$_2$	0.04607	0.0039
−0.5	0.1 M K$_2$SO$_4$ with O$_2$	−0.043	−0.0036
1	0.1 M K$_2$SO$_4$ no O$_2$	0.03421	0.0029
−0.5	0.1 M K$_2$SO$_4$ no O$_2$	−0.04374	−0.0037

S13. Application of +1.0 V results in no change to sulfate activity

Difference spectra were recorded relative to electrode equilibrated for 30 min without applied potential. Resulting spectra show that only −0.5 V and not +1.0 V results in a change in the sulfate band. The potential step duration was kept at 720 seconds and four sample spectra were recorded during the initial 600 seconds in order to keep all other experimental parameters as similar as possible to all other experiments reported.
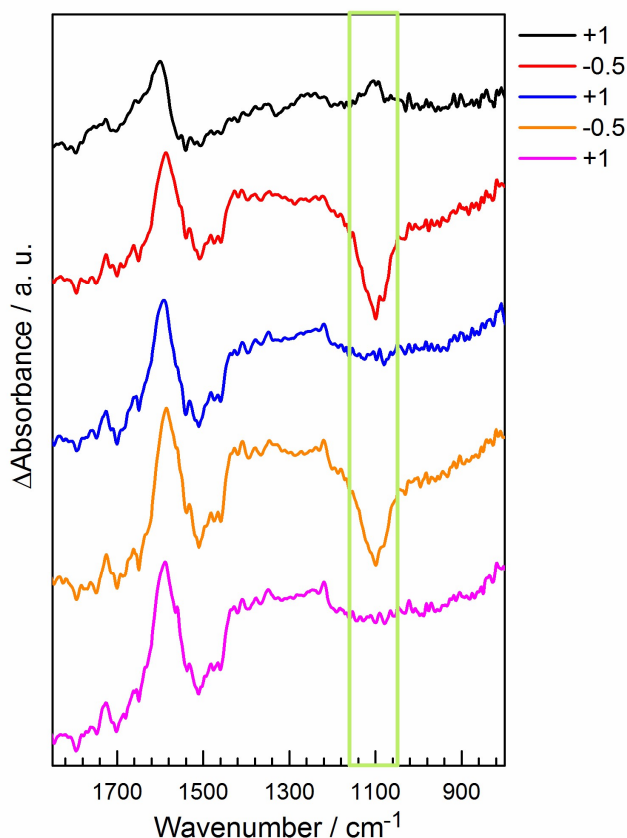
Figure S13. Difference spectra of BDD modified with GNF-Ca in 0.1 M Na$_2$SO$_4$ pH 6.8. Background recorded at the beginning of experiment before the application of potential. Potentials: +1 V (black); −0.5 V (red); +1 V (blue); −0.5 V (orange); +1 V (pink). The sulfate band at 1100 cm^{-1} is highlighted in green.

S14. Preconcentration of sulfate at GNF-Ca electrode prior to application of potential
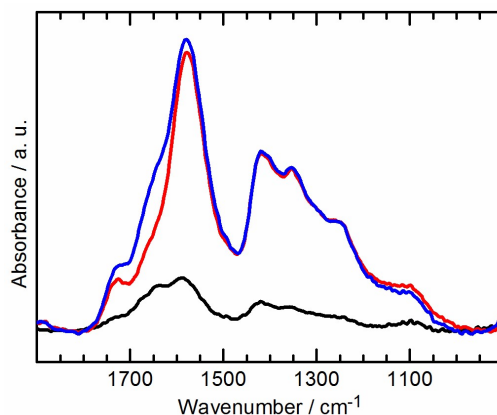
Figure S14. IR spectra of GNF-Ca modified BDD electrode after immersion into 0.1 M K$_2$SO$_4$ electrolyte at pH 6.8. Immediately after insertion (black), 5 minutes after insertion (red), 35 minutes after insertion (blue). Peak fit of sulfate band corresponds to 7.6 × 10^{-3} mol dm^{-3} sulfate.

Over the first 5 mins of immersion in electrolyte the spectral intensity of the GNF-Ca increases as the electrolyte penetrates the porous layer and causes it to swell. Swelling of the layer allows the GNF-Ca to occupy the whole region between the BDD electrodes and the ATR prism and more of the layer is probed by the evanescent IR radiation, hence spectral intensity is increased.

The band at 1100 cm^{-1} can be attributed to SO$_4^{2-}$ ions that are present in the swollen hydrated layers at higher concentrations than in the background electrolyte. Peak fitting of this band and comparison of its area with the calibration curve in S12 allows us to approximate that the excess SO$_4^{2-}$ concentration within the GNF-Ca layer is *ca*. 7 x 10^{-3} mol dm^{-3}.

S15. Effect of different applied potentials on spectral response

Data was recorded with variable electrode potentials and these show the same trends as observed for +1.0 V and -0.5 V, but less extreme potentials cause smaller changes in the absorbance bands. The potentials used in the main manuscript were therefore chosen such that the observed changes were as intense as possible without exceeding the solvent stability window (see CV in Figure S9.1) for the potential window of the modified electrode.
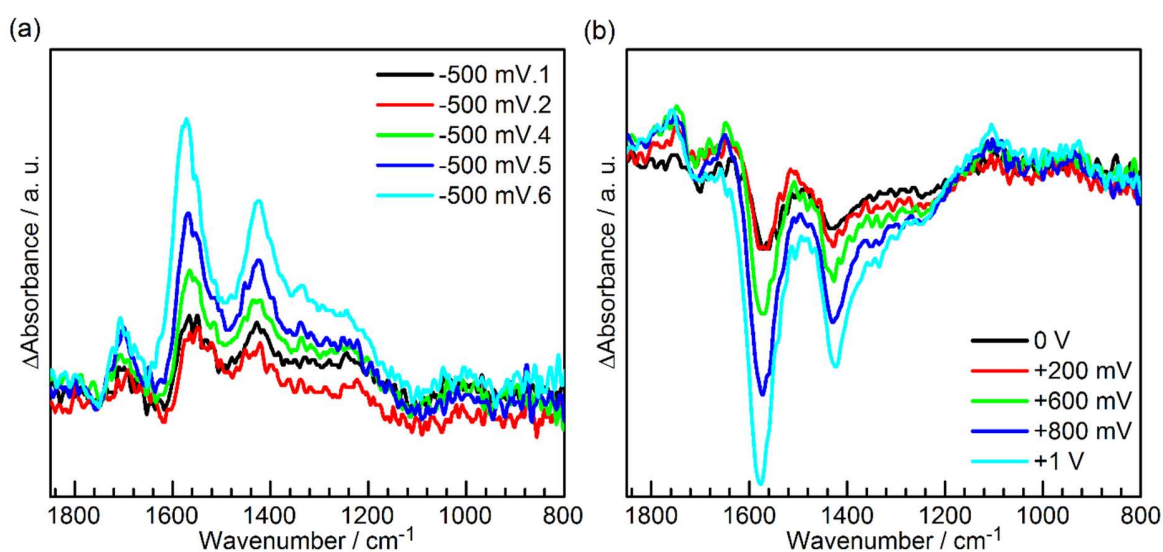
Figure 15: ATR IR difference spectra of the GNF-Ca modified electrode interface in 0.1 M pH 7 Na$_2$SO$_4$. Panel (a): application of −0.5 V after background was collected at 0 V (black), +0.2 V (red), +0.6 V (green), +0.8 V (blue), +1 V (light blue). Panel (b): application of variable positive potential after background was collected at −0.5 V: 0 V (black), +0.2 V (red), +0.6 V (green), +0.8 V (blue), +1 V (light blue).

S16. Calculation of the values presented in Tables 1 and 2

<u>All calculations assume that activity coefficients = 1</u>

<u>0.1 M pH 7 K_2SO_4 solution</u>

Stoichiometry: 0.1 $K_2SO_4 \rightarrow$ 0.2 K^+ + 0.1 SO_4^{2-}

As $pK_a(HSO_4^-)$ = 1.92, at pH 7 all sulfate species are present as SO_4^{2-} and cannot be protonated by any realistic increase in a_{K+}. Therefore, any change in a_{SO42-} on application of −0.5 V represents ion migration only.

At equilibrium and +1.0 V assume:

 a_{SO42-} = 0.100 a_{K+} = 0.200

[For simplicity neglecting the increased sulfate concentration at the interface due to pre-concentration (it is clear from IR spectra in Fig S14 that a_{SO42-} is higher at the electrode interface than in the bulk solution by *ca*. 7 x 10^{-3} mol dm^{-3})]

From calibration experiments in Section S12, on application of −0.5 V, due to migration effects:

Δ_{aSO42-} = −3.5 × 10^{-3}

So we can assume that on application of −0.5 V: Δa_{K+} = +7 × 10^{-3}

<u>0.1 M pH 3.5 K_2SO_4 solution</u>

pH 3.5 K_2SO_4 was prepared by addition of 0.1 M H_2SO_4 to 0.1 M K_2SO_4 with the following stoichiometry:

0.098 K_2SO_4 + 0.002 $H_2SO_4 \rightarrow$ 0.198 K^+ + 0.097 SO_4^{2-} + 0.003 HSO_4^-

Therefore, at equilibrium and 1.0 V: a_{K+} = 0.198

On application of −0.5 V: a_{K+} = 0.205

Using Eq 1: $pK_a(app) = pK_a + pK_{as} - \log(a_{K+})$

          Where $pK_a(HSO_4^-)$ = 1.92 and assuming pK_{as} = 0

At equilibrium: $pK_a(app) = 1.92 + 0 - \log(0.198) = 2.623$

At -0.5 V: $\quad pK_a(app) = 1.92 + 0 - \log(0.205) = 2.608$

These values of $pK_a(app)$ along with the Henderson-Hasselbalch equation can be used to determine the speciation at a specific pH:

$pH = pK_a(app) + \log\{a_{SO_4^{2-}}/a_{HSO_4^-}\}$

Therefore, for pH 3.5 solution on application of -0.5 V: $\quad \underline{\Delta a_{SO_4^{2-}} = +0.35 \times 10^{-3} \text{ mol dm}^{-3}}$

<u>0.1 M pH 3 K_2SO_4 solution</u>

Prepared with the following stoichiometry:

$$0.096 \ K_2SO_4 + 0.004 \ H_2SO_4 \rightarrow 0.192 \ K^+ + 0.092 \ SO_4^{2-} + 0.008 \ HSO_4^{2-}$$

Therefore, at equilibrium and 1.0 V: $a_{K^+} = 0.192$ mol dm^{-3} $pK_a(app) = 2.637$

On application of -0.5 V: $\quad a_{K^+} = 0.199$ mol dm^{-3} $pK_a(app) = 2.621$

Corresponds to a $\underline{\Delta a_{SO_4^{2-}} = +0.75 \times 10^{-3} \text{ mol dm}^{-3}}$

<u>0.1 M pH 7 phosphate</u>

$$0.05 \ K_2HPO_4 + 0.05 \ KH_2PO_4 \rightarrow 0.15 \ K^+ + 0.05 \ HPO_4^{2-} + 0.05 \ H_2PO_4^-$$
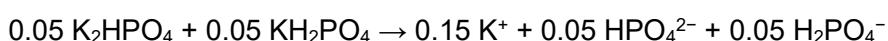
Using: $\quad pK_a(H_2PO_4^-) = 7.2 \quad pK_{as} = 0$

Therefore, at equilibrium and 1.0 V: $a_{K^+} = 0.150$ mol dm^{-3} $pK_a(app) = 8.024$

On application of -0.5 V: $\quad a_{K^+} = 0.157$ mol dm^{-3} $pK_a(app) = 8.004$

Corresponds to a $\underline{\Delta a_{HPO_4^{2-}} = +0.37 \times 10^{-3} \text{ mol dm}^{-3}}$

<u>0.1 M pH 9 phosphate</u>

$$0.1 \ K_2HPO_4 \rightarrow 0.2 \ K^+ + 0.1 \ HPO_4^{2-}$$

Using: $pK_a(H_2PO_4^-) = 7.2$ $pK_{as} = 0$

Therefore, at equilibrium and 1.0 V: $a_{K+} = 0.200$ mol dm^{-3} $pK_a(app) = 8.024$

On application of −0.5 V: $a_{K+} = 0.207$ mol dm^{-3} $pK_a(app) = 8.004$

Corresponds to a $\underline{\Delta a_{HPO42^-} = +0.23 \times 10^{-3}}$ mol dm^{-3}

<u>pH 3 phosphate</u>

      $0.02\ H_3PO_4 + 0.08\ KH_2PO_4 \rightarrow 0.08\ K^+ + 0.01\ H_3PO_4 + 0.09\ H_2PO_4^-$

Using: $pK_a(H_3PO_4) = 2.12$ $pK_{as} = 0$

Therefore, at equilibrium and 1.0 V: $a_{K+} = 0.080$ mol dm^{-3} $pK_a(app) = 3.217$

On application of −0.5 V: $a_{K+} = 0.087$ mol dm^{-3} $pK_a(app) = 3.180$

Corresponds to a $\underline{\Delta a_{HPO42^-} = +2.0 \times 10^{-3}}$ mol dm^{-3}

S17. Estimating the number of acid groups undergoing potential-induced changes

3.3×10^{-3} g of dry acid-terminated GNF was used to prepare GNF-Ca precipitate. The number of acidic protons has previously been estimated to be 7×10^{-3} mol per gram of GNF. The total number of both protonated and deprotonated carboxylate groups present on the electrode is therefore estimated to be 1.26×10^{-7} mol. However, it is unclear what fraction of carboxylate groups in GNF-Ca are complexed with divalent Ca^{2+} and how many groups remain non-complexed and therefore available to contribute to the potential-dependent spectral features. To estimate the number of non-complexed COO^-/COOH groups at the electrode surface undergoing potential-induced changes, the peak areas in potential difference spectra were compared with those of a simple carboxylic acid (acetic acid). Because the GNF acid groups are bound to the surface, calibration using an aqueous acid at different concentrations was deemed inapplicable and hence a calibration curve was constructed using varying amounts of a dried deprotonated acetic acid (acetate) deposited on the ATR prism to mimic a surface layer.

Acetic acid solutions of different concentrations were prepared and the pH was adjusted with potassium hydroxide to deprotonate all acid groups. A background of the clean ATR prism was collected and 1×10^{-6} l of each solution was pipetted onto the prism and allowed to dry before recording a sample spectrum. The carboxylate stretches were fitted with Gaussian peak shapes and the peak areas were plotted against the number of moles in each sample. The data points were fitted with a linear equation, the intercept of which was fixed to zero to ensure physically meaningful estimations of small numbers of moles from the calibration curve (Fig S17.1).

Because the number of groups undergoing changes is estimated based on peak areas in IR spectra, the number obtained is dependent on the distance to the IRE. The dry potassium acetate film is very thin (thinner than the penetration depth, see S5) and it can therefore be assumed that the signal represents the total sample amount. However, when IR spectra are recorded of the thick GNF-Ca layer at the electrode surface, the signal isn't a straightforward reflection of the total number of acidic groups due to the exponential decay of the evanescent wave's electric field.

(a)

(b)

(c)
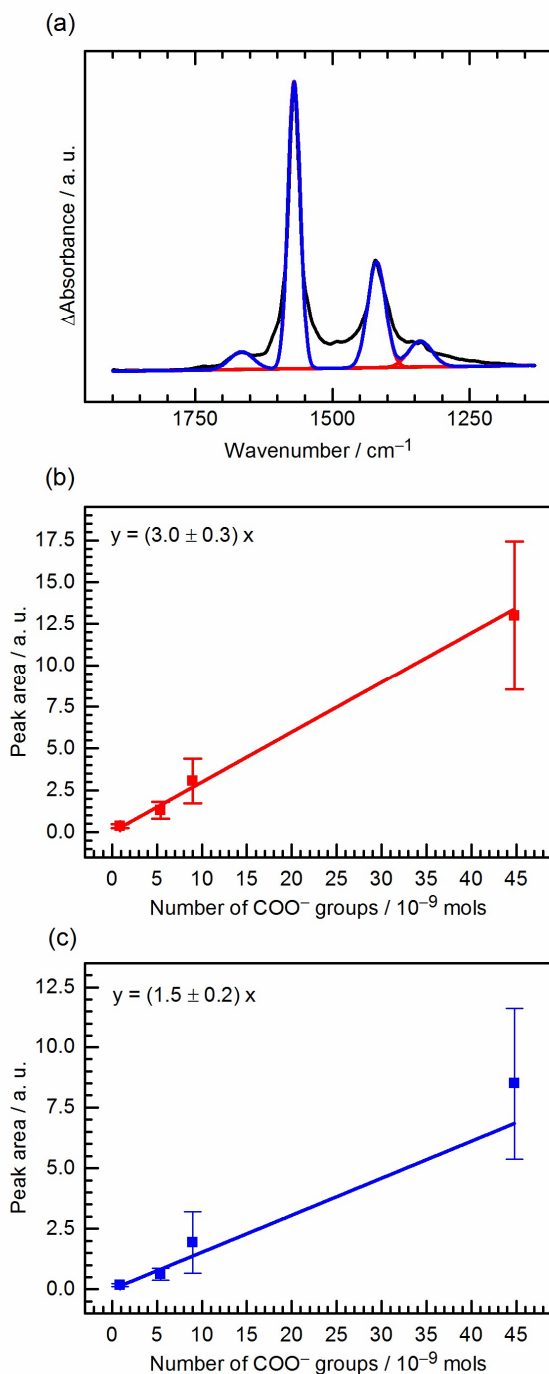
Figure S17.1 (a) Peak fit of dropcast potassium acetate film containing 5.38 × 10⁻⁹ moles of acetate groups. Experimental data (black), background (green), peak fits (red), cumulative peak fit (blue). (b) Asymmetric stretch peak areas at 1565 cm⁻¹ plotted against number of acetate groups and a linear fit of data points. (c) Symmetric stretch peak areas at 1565 cm⁻¹ plotted against number of acetate groups and a linear fit of data points.

Supporting Information

We can estimate the number of groups dissociating under applied potential by adjusting the peak areas in the difference spectra by the relationship of the effective penetration depth, d_{ep} (see section S5) and the thickness of the GNF-Ca film, h, which is taken to be 17 µm as calculated in Section S4. The adjusted peak areas were then compared to the calibration curve to estimate the number of carboxylate groups lost and gained due to potential-induced protonation and deprotonation.

Figure S17.2 shows an example of peak fitted difference spectrum for the GNF-Ca in 0.1 M K_2SO_4 pH 6.8. Peaks used in estimating the number of carboxylate groups were the asymmetric peak at 1570 cm^{-1} and the symmetric peak at 1430 cm^{-1}, and spectra from three separate experiments in 0.1 M K_2SO_4 pH 6.8 were evaluated, both with and without oxygen present in solution. The average areas found from the difference spectra were 0.034 and 0.023 for the asymmetric and symmetric peaks, respectively. These were adjusted by the ratio d_{ep}/h, at each wavelength, giving adjusted peak areas of 0.3 ± 0.2 and 0.2 ± 0.1 for the asymmetric and symmetric peaks, respectively.

From the adjusted peak areas, the number of carboxylate groups changing protonation state has been evaluated as (1.5 ± 0.6) × 10^{-9} mol using the linear regression lines in Fig S17.1 b and c. The peak areas are listed in Table S17.1.
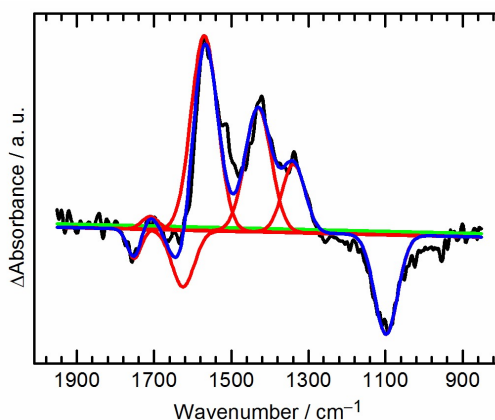
Figure S17.2 Peak fitted difference spectrum in 0.1 M K_2SO_4 pH 6.8 when applying −0.5 V to GNF-Ca modified BDD. Experimental data (black), background curve (green), peak fits (red), cumulative peak fit (blue).

Table S17.1 Carboxylate asymmetric and symmetric stretch peak areas from difference spectra obtained at different potentials.

Potential / V	Conditions	$v_{as}(COO^-)$ peak area	$v_s(COO^-)$ peak area
1	0.1 M K_2SO_4 with O_2	0.03264	0.02016
−0.5	0.1 M K_2SO_4 with O_2	−0.04529	−0.02611
1	0.1 M K_2SO_4 with O_2	0.00965	0.00882
−0.5	0.1 M K_2SO_4 with O_2	−0.02314	−0.01494
1	0.1 M K_2SO_4 no O_2	0.05816	0.04429
−0.5	0.1 M K_2SO_4 no O_2	−0.09869	−0.05678

Using Eq.1 and the Henderson-Hasselbalch equation we can calculate what percentage of the total number of GNF-COOH groups this value of $(1.5 \pm 0.6) \times 10^{-9}$ mol corresponds to. In our estimate of $pK_a(app)$ we assume that the pK_a of carboxylic acid groups is 3 and that the pK_{as} of COOK is 0.5. These values are estimates but the actual values do not affect the relative resulting $pK_a(app)$ in switching to −0.5 V. As for the calculations in Section S16 was assume a_M+ changes from 0.2 M at equilibrium to 0.207 M when a negative potential is applied. The ratio $[COO^-]/[COOH]$ at pH 6.8 is then calculated using the Henderson–Hasselbalch equation. Using these values, the <u>change in the number of COO^- at −0.5 V compared to equilibrium is found to be +3.5%.</u>

Table S17.2 Values used to calculate change in the number of carboxylate groups at the electrode surface when a potential is applied.

Potential / V	a_M+	$pK_a(app) =$ $pK_a + pK_{as} - \log(a_M+)$	$[COO^-]/[COOH] =$ $10\text{^}(pH-pKa(app))$
Equilibrium	0.2	4.20	399
−0.5	0.207	4.18	413

This calculated 3.5% increase in GNF-COO$^-$ at -0.5 V corresponds to $(1.5 \pm 0.6) \times 10^{-9}$ mol of carboxylate, as determined from IR peak area.

Because this number represents 3.5% of non-complexed groups, the total number of non-complexed COO$^-$/COOH groups is estimated to be $((1.5 \pm 0.6) \times 10^{-9}) / 0.035 = (4 \pm 2) \times 10^{-8}$ mols.

As the total number of COO$^-$/COOH groups prior to complexation is calculated as 1.26×10^{-7} mol, $(4 \pm 2) \times 10^{-8}$ mol corresponds to (35 ± 14) % of all COO$^-$/COOH groups that remain non-complexed.